Disruption of Glycosylphosphatidylinositol-Anchored Lipid Transfer Protein Gene Altered Cuticular Lipid Composition, Increased Plastoglobules, and Enhanced Susceptibility to Infection by the Fungal Pathogen *Alternaria brassicicola*[1][W]

Saet Buyl Lee, Young Sam Go, Hyun-Jong Bae, Jong Ho Park, Sung Ho Cho, Hong Joo Cho, Dong Sook Lee, Ohkmae K. Park, Inhwan Hwang, and Mi Chung Suh*

Department of Plant Biotechnology and Agricultural Plant Stress Research Center (S.B.L., Y.S.G., M.C.S.) and Department of Wood Science and Technology (H.-J.B.), College of Agriculture and Life Sciences, Chonnam National University, Gwangju 500–757, Republic of Korea; Department of Biological Sciences, Inha University, Incheon 402–751, Republic of Korea (J.H.P., S.H.C.); School of Life Sciences and Biotechnology, Korea University, Seoul 136–701, Republic of Korea (H.J.C., D.S.L., O.K.P.); and Division of Molecular and Life Sciences, Pohang University of Science and Technology, Pohang 790–784, Republic of Korea (I.H.)

All aerial parts of vascular plants are covered with cuticular waxes, which are synthesized by extensive export of intracellular lipids from epidermal cells to the surface. Although it has been suggested that plant lipid transfer proteins (LTPs) are involved in cuticular lipid transport, the in planta evidence is still not clear. In this study, a glycosylphosphatidylinositol-anchored LTP (*LTPG1*) showing higher expression in epidermal peels of stems than in stems was identified from an Arabidopsis (*Arabidopsis thaliana*) genome-wide microarray analysis. The expression of *LTPG1* was observed in various tissues, including the epidermis, stem cortex, vascular bundles, mesophyll cells, root tips, pollen, and early-developing seeds. LTPG1 was found to be localized in the plasma membrane. Disruption of the *LTPG1* gene caused alterations of cuticular lipid composition, but no significant changes on total wax and cutin monomer loads were seen. The largest reduction (10 mass %) in the *ltpg1* mutant was observed in the C29 alkane, which is the major component of cuticular waxes in the stems and siliques. The reduced content was overcome by increases of the C29 secondary alcohols and C29 ketone wax loads. The ultrastructure analysis of *ltpg1* showed a more diffuse cuticular layer structure, protrusions of the cytoplasm into the vacuole in the epidermis, and an increase of plastoglobules in the stem cortex and leaf mesophyll cells. Furthermore, the *ltpg1* mutant was more susceptible to infection by the fungus *Alternaria brassicicola* than the wild type. Taken together, these results indicated that LTPG1 contributed either directly or indirectly to cuticular lipid accumulation.

During growth and development, plants are subjected to various environmental stresses, including drought, cold, exposure to UV light, and pathogen attack. The first barrier between plants and environmental stresses is the cuticle, which is composed of a lipophilic cutin polymer matrix and waxes (Holloway, 1982; Jeffree, 1996; Kunst et al., 2005; Nawrath, 2006). The cuticular waxes, which consist of very long chain fatty acids (VLCFAs; C20 to C34) and their derivatives, are embedded within and encase the cutin polymer matrix, a polyester framework composed of hydroxy fatty acids (C16 and C18) and glycerol monomers (Kolattukudy, 2001; Jenks et al., 2002; Nawrath, 2002; Heredia, 2003; Kunst and Samuels, 2003; Stark and Tian, 2006). The cuticle plays a role in limiting nonstomatal water loss and gas exchange, repelling lipophilic pathogenic spores and dust, providing mechanical strength and viscoelastic properties (Baker et al., 1982; Hoffmann-Benning and Kende, 1994; Riederer and Schreiber, 2001), preventing cell fusions (Lolle et al., 1998; Sieber et al., 2000), and protecting plants from environmental stresses (Schweizer et al., 1996).

It has been suggested that the biosynthesis of cuticular wax occurs exclusively within epidermal cells (Kunst and Samuels, 2003; Suh et al., 2005). During this process, the C16 and C18 fatty acids synthesized in the plastids are exported to the cytosol, where they are further elongated to VLCFAs in the range of 20 to 34 carbons by the fatty acid elongase complex on the endoplasmic reticulum (ER; Millar and Kunst, 1997; Millar et al., 1999; Todd et al., 1999; Yephremov et al.,

[1] This work was supported by the Agricultural Plant Stress Research Center (grant no. R11–2001–09205001–0 to M.C.S.) and the Interdisciplinary Research Program (grant no. R01–2006–000–11056–02008 to M.C.S.) of the Korea Science and Engineering Foundation, Republic of Korea.

* Corresponding author; e-mail mcsuh@chonnam.ac.kr.

The author responsible for distribution of materials integral to the findings presented in this article in accordance with the policy described in the Instructions for Authors (www.plantphysiol.org) is: Mi Chung Suh (mcsuh@chonnam.ac.kr).

[W] The online version of this article contains Web-only data.
www.plantphysiol.org/cgi/doi/10.1104/pp.109.137745

1999; Fiebig et al., 2000; Clemens and Kunst, 2001; Hooker et al., 2002; Dietrich et al., 2005; Zheng et al., 2005). The elongated VLCFAs are then further transformed by two principal wax biosynthetic pathways: an acyl reduction pathway that produces primary alcohols and wax esters, and a decarbonylation pathway that leads to the formation of aldehydes, alkanes, secondary alcohols, and ketones (Aarts et al., 1995; Kunst and Samuels, 2003; Rowland et al., 2006). It has been suggested that the synthesized wax precursors are then exported from their site of synthesis in the ER to their site of deposition on the plant outer surface by a vesicular pathway (Schulz and Frommer, 2004). Recently, it was reported that ATP-binding cassette (ABC) transporters, which are located in plasma membrane of the epidermis, are required for cuticular lipid export (Pighin et al., 2004; Bird et al., 2007; Luo et al., 2007).

Lipid transfer proteins (LTPs) were initially defined by their ability to facilitate the transfer of phospholipids between membranes in vitro and in vivo (Kader, 1996). Plant LTPs are small (7–10 kD), abundant, and basic proteins that have a hydrophobic pocket capable of accommodating fatty acids or lysophospholipid molecules (Shin et al., 1995; Beisson et al., 2003). The results of plant genome and EST projects have demonstrated the presence of multiple LTP isoforms, which are speculated to be associated with diverse functions including cutin and wax assembly, pathogen defense, antifreezing, long-distance signaling, and cell wall loosening (Pyee and Kolattukudy, 1995; Molina and García-Olmedo, 1997; Maldonado et al., 2002; Beisson et al., 2003; Jeroen et al., 2005; Cameron et al., 2006; Roy-Barman et al., 2006; Choi et al., 2008). Most plant LTPs localize to the cell wall, which suggests that LTPs play a role in cutin monomers and wax transport (Pyee and Kolattukudy, 1995). The accumulation of cuticular wax on the leaves of tree tobacco (*Nicotiana glauca*) and the concomitant increase in LTP expression in response to drought stress indirectly suggest that LTP is involved in the accumulation of wax (Cameron et al., 2006).

Recently, proteomic analysis identified 26 Arabidopsis (*Arabidopsis thaliana*) LTP-like proteins that contained the glycosylphosphatidylinositol (GPI)-anchored domain (Borner et al., 2003); however, the functions of these proteins still remain to be investigated. It is known that GPI-anchored proteins are attached to the outer surface of the plasma membrane via a GPI anchor. In diverse organisms from protozoa to vertebrates, GPI anchoring is processed in the ER lumen by cleavage of the C-terminal carboxyl group of a protein and subsequent addition of a core structure composed of ethanolamine phosphate, trimannoside, glucosamine, and inositol phospholipid (Udenfriend and Kodukula, 1995). GPI anchors have been implicated in plasma membrane targeting, polarized targeting of the apical plasma membrane, associations with lipid rafts, recycling of the plasma membrane, and the reception and transduction of signals (Mayor and Riezman, 2004).

In a previous report (Suh et al., 2005), transcriptome analysis of Arabidopsis stems and stem epidermal cells was conducted to identify genes involved in surface lipid metabolism. This analysis identified seven LTP candidates that might play a role in wax and/or cutin monomer transport. In this study, *LTPG1* (At1g27950), which showed higher expression in the epidermal peels of stems than in the stems, was selected based on an unusual LTP structure containing a long C-terminal region, whose function has not been well characterized. Spatial and temporal expression of the *LTPG1* gene and subcellular localization of the LTPG1 protein were then investigated. In addition, a T-DNA-inserted *atltpg-1* knockout mutant was characterized to evaluate the role of LTPG1 in planta.

RESULTS

Isolation of the *LTPG1* Gene Encoding GPI-Anchored LTP

To confirm the expression levels of the *LTPG1* transcripts in the stems and stem epidermal peels, the total RNA was isolated and subjected to reverse transcription (RT)-PCR and quantitative real-time RT-PCR analyses. The Arabidopsis *actin2* gene (At3g18780) was then used to determine the quantity and quality of the cDNAs. Similar to the microarray results, the expression levels of the *LTPG1* transcripts were approximately 2.5-fold higher in the stem epidermal peels than in the stems (Fig. 1, A and B).

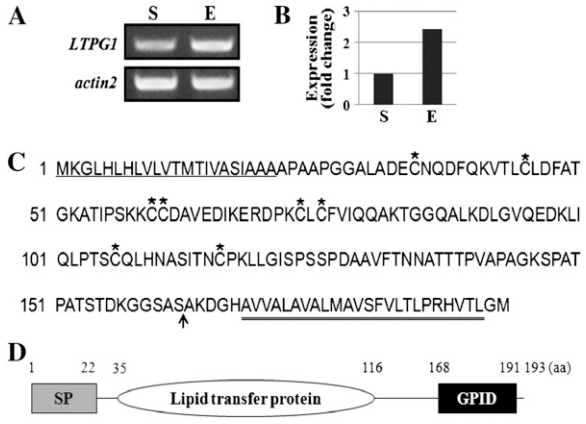

Figure 1. Isolation of the *LTPG1* gene. A and B, Expression of the *LTPG1* transcripts in stems (S) and stem epidermal peels (E). Total RNA (0.1 μg) was used for RT-PCR (A) and quantitative RT-PCR (B) analyses. The *actin2* gene (At3g18780) was used to determine the quantity and quality of the cDNA. Each value in B is the mean of duplicate experiments. C, Amino acid sequences of the LTPG1 protein. Asterisks denote the conserved Cys residues. The signal peptide domain and GPI-anchored domain are underlined and double underlined, respectively. The arrow indicates the EYFP insertion site for subcellular localization of LTPG1. D, Schematic diagram of the LTPG1 protein. GPID, GPI-anchored domain; SP, signal peptide domain.

The LTPG1 protein was found to contain three different domains. Specifically, 22 amino acid residues at the N terminus were found to correspond to a signal peptide predicted to be required for protein secretion. In addition, the amino acid residues located between residues 35 and 116, which are approximately 60% homologous with nonspecific LTP, were found to harbor eight highly conserved Cys residues at positions 35, 45, 60, 61, 74, 76, 106, and 116. Finally, the C-terminal end (residues 168–191) contained a sequence that was predicted to encode the GPI-anchored domain (Fig. 1, C and D).

Spatial and Temporal Expression of the *LTPG1* Transcripts

To investigate the expression of the *LTPG1* transcripts, the total RNA was isolated from the roots, young seedlings, leaves, caulines, flowers, and siliques and then subjected to RT-PCR analysis. The *LTPG1* transcripts were expressed in all of the tissues tested (Supplemental Fig. S1A). The expression levels of the *LTPG1* transcripts were then further evaluated to determine if they were regulated by abiotic stresses and the stress hormone abscisic acid (ABA). To accomplish this, 10-d-old seedlings were incubated in Murashige and Skoog (MS) medium that had been supplemented with 200 mM NaCl, 200 mM mannitol, 20% polyethylene glycol, or 1 μM ABA, and RT-PCR was conducted. The *actin7* (At5g09810) gene was used to determine the quantity and quality of the cDNAs. The *rd29A* gene (At5g52310), which is known to be a drought stress-inducible gene, was used as a control for the water-deficit response. Expression of the *rd29A* gene increased significantly in response to treatment, whereas the level of *LTPG1* transcripts was not affected by ABA, salt, or osmotic stress (Supplemental Fig. S1B).

The spatial and temporal expression of the *LTPG1* gene was further evaluated by introducing the bacterial *uidA* gene under the promoter region of the *LTPG1* gene into Arabidopsis plants. Tissue samples of five independent transgenic lines were then stained for GUS activity. The GUS gene under the promoter region of the *LTPG1* gene was strongly expressed in the aerial portion of the 10-d-old seedlings. In addition, GUS expression was observed in the root tips, upper portion of the styles, pollen, and veins of the sepals and petals. Furthermore, the silique walls and seeds in the early stages of development (before the seeds turned brown) were stained. When the stem and leaf tissues were cross-sectioned, the GUS gene was found to be expressed in the stem and leaf epidermis, including the trichomes, leaf mesophyll cells, and stem cortex and xylem (Fig. 2).

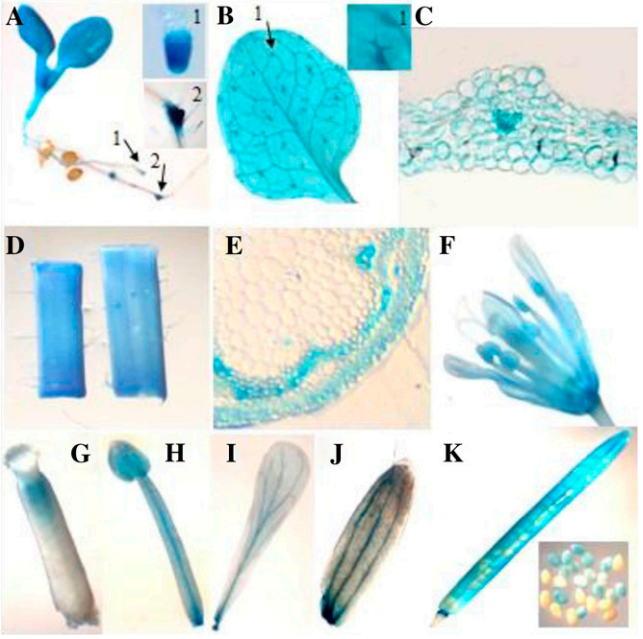

Figure 2. GUS expression under the *LTPG1* promoter in transgenic Arabidopsis plants. The *LTPG1* promoter::GUS construct was transformed into Arabidopsis plants, and five independent transgenic lines were then stained with 1 mM 5-bromo-4-chloro-3-indolyl-β-D-glucuronide. A, Ten-day-old seedling. High magnification of the root tip (inset 1) and initiation site of lateral roots (inset 2) are indicated by arrows. B, Two-week-old leaf. High magnification of a trichome (inset 1) is indicated by the arrow. C, Cross-section of a leaf. D, Stem. E, Cross-section of a stem. F, Flower. G, Carpel. H, Stamen. I, Petal. J, Sepal. K, Silique wall and developing seeds.

LTPG1 Protein Is Localized in the Plasma Membrane

GPI-anchored proteins are mainly found on the plasma membrane (Udenfriend and Kodukula, 1995), and LTPG1 harbors the GPI-anchored domain at its C-terminal end; therefore, subcellular localization of LTPG1 was investigated. To accomplish this, the enhanced yellow fluorescent protein (EYFP) protein was inserted between the LTP domain and the GPI-anchored domain (between amino acid residues 162 and 163), after which the resulting construct and control plasmids with no targeting signals were introduced into Arabidopsis protoplasts. When Arabidopsis protoplasts transformed with the LTPG1:EYFP construct were visualized with a fluorescence microscope, fluorescent signals were observed in the plasma membrane (Fig. 3, A and B). However, the fluorescent signals from Arabidopsis protoplasts that had been transformed with the control EYFP construct were detected in the cytosol (Fig. 3, C and D). This result was confirmed by introducing the LTPG1:EYFP construct into tobacco epidermis via *Agrobacterium tumefaciens* infiltration (Fig. 3, E–H).

The role of the GPI-anchored domain in targeting the LTPG1 protein to the plasma membrane was also investigated in the protoplast system. To accomplish this, red fluorescent protein (RFP) was fused to the C-terminal end of the LTPG1 protein after deletion of 48 amino acids (residues 145–193), including the GPI-

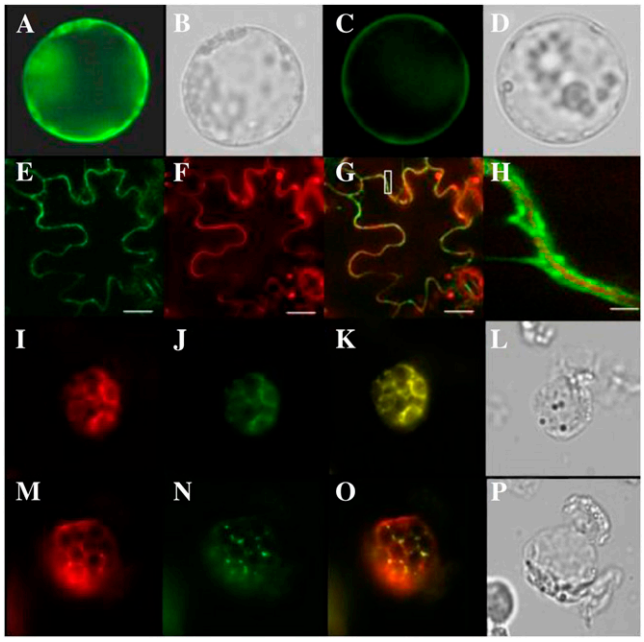

Figure 3. LTPG1:EYFP is localized in the plasma membrane of the Arabidopsis protoplast and tobacco epidermal cells. Arabidopsis protoplasts (A–D and I–P) and tobacco epidermis (E–H) transformed with each construct were visualized with a fluorescence microscope (Nikon Eclipse TE2000-U) and a laser confocal scanning microscope (TCS SP5 AOB5/Tandem; Leica), respectively. A and B, Control, p35S-EYFP-Flag/Strep plasmid. C to E, LTPG1:EYFP construct. F, Propidium iodide staining to visualize the cell wall. G, Merged images from E and F. H, Magnification of the inset box in G. I and M, LTPG1:RFPΔ48 construct. J, Bip:GFP construct. K, Merged images from I and J. N, ST:GFP construct. O, Merged images from M and N. Images were acquired through a GFP filter (A, C, E, J, and N), an RFP filter (F, I, and M), or a bright fields (B, D, L, and P). Bars = 25 μm (E–G) and 2.5 μm (H).

anchored domain, from the C-terminal end. When the resultant construct, LTPG1Δ48:RFP, was cointroduced into protoplasts with the *Bip*:*GFP* construct as an ER maker or the *ST*:*GFP* construct as a Golgi marker (Min et al., 2007), the red fluorescent signals were colocalized with the Bip:GFP signals (Fig. 3, I–L) but not with the ST:GFP signals (Fig. 3, M–P). Taken together, these results indicate that the LTPG1 protein is localized to the plasma membrane and that GPI anchoring is essential for the LTPG1 protein to leave the ER.

Isolation of the T-DNA-Tagged *ltpg1* Knockout Mutant

To examine the roles that the *LTPG1* gene plays in planta, a T-DNA-tagged *atltpg-1* (Garlic_1166_G01.b.1a.Lb3Fa) Arabidopsis mutant was obtained from the Syngenta Arabidopsis Insertion Library resources (Fig. 4A). The seeds were then germinated on half-strength MS agar medium supplemented with phosphinothricin, after which PCR screening was conducted to amplify a product specific for the DNA sequence flanking a T-DNA insertion in the *LTPG1* coding region.

Screening of the Garlic_1166_G01.b.1a.Lb3Fa line using the left border (LB1) and the LTPG1 cDNA F2 primers yielded PCR products consistent with a T-DNA insertion in the second exon of the *LTPG1* gene. However, no PCR products were observed when this primer set was used to amplify DNA from wild-type plants. In addition, when PCR was conducted using the LTPG1 cDNA F2 and LTPG1 cDNA R2 primers, PCR products corresponding to the coding region and an intron of the *LTPG1* gene were detected in the wild type but not in the Garlic_1166_G01.b.1a.Lb3Fa line (Fig. 4B). Finally, when the phosphinothricin-resistant Garlic_1166_G01.b.1a.Lb3Fa line was back-crossed with the wild type and analyzed for phosphinothricin resistance, the F2 progeny from the three independent lines were segregated approximately 3:1 (resistant: sensitive; Supplemental Table S1). These results revealed that the isolated Garlic_1166_G01.b.1a.Lb3Fa line (*ltpg1*) is a homozygote that carries T-DNA insertions in the second exon of the *LTPG1* gene and that a single copy of the T-DNA was integrated into the *LTPG1* gene.

To evaluate the mRNA expression of the *LTPG1* gene in the *ltpg1* mutant, the total RNA was isolated from 10-d-old wild-type and *ltpg1* mutant seedlings and then subjected to RT-PCR analysis. As shown in Figure 4C, the wild-type RNA contained full-length *LTPG1* transcripts, while the *ltpg1* mutant did not contain any detectable *LTPG1* transcripts. The *ltpg1* knockout mutants grew and developed normally when compared with the wild-type plants under regular growth conditions.

Cuticular Lipid Composition Is Altered in the *ltpg1* Mutant

It has been suggested that LTPs are involved in the transport of waxes or cutin monomers (Kader, 1996); therefore, disruption of the *LTPG1* gene was first

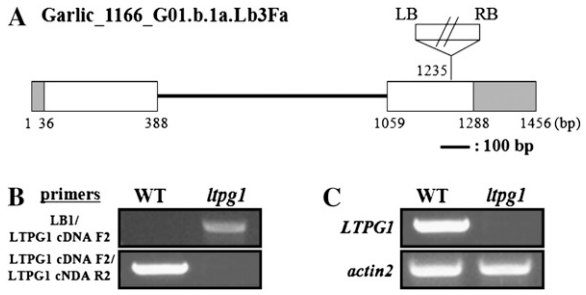

Figure 4. Isolation of T-DNA-tagged *ltpg1* mutant. A, Genomic organization of a T-DNA-tagged *LTPG1* gene. *LTPG1* genomic DNA is represented by two exons in the white box, an intron in the black line, and untranslated regions in the gray box. The T-DNA orientation is indicated by the left (LB) and right (RB) borders. B, Genomic DNA isolated from the wild type (WT) and the *ltpg1* mutant was subjected to PCR. C, RT-PCR analysis of the *LTPG1* gene in wild-type and *ltpg1* mutant plants. Total RNA (0.2 μg) was used to detect the *LTPG1* transcripts.

evaluated to determine if it caused alterations in the composition and amount of extracellular lipids. To accomplish this, the cuticular waxes extracted from the stems, siliques, and leaves of wild-type and *ltpg1* mutant plants were analyzed using gas chromatography-mass spectrometry (GC-MS) and GC. The largest reduction (10 mass %) in the mutant was observed in the C29 alkane (nonacosane), which is the major component of cuticular waxes in the stems and siliques. The reduced content was overcome by increases of C29 secondary alcohol and C29 ketone wax loads (Fig. 5A). A similar observation was made in the siliques but interestingly not in the leaves (Fig. 5, B and C). In addition, C28 aldehyde, C27 alkane, and C24 primary alcohol in stems, C28 fatty acid, C28 aldehyde, C27 alkane, and C24 and C26 primary alcohols in siliques, and C28 aldehyde, C26 primary alcohol, and C27 alkane in leaves were reduced to less than 5 mass % in each tissue. Approximately 2 mass % of C33 alkane was increased in leaves (Fig. 5, A–C). However, no significant alteration was observed in the total wax load of *ltpg1* stems and leaves (Fig. 5, D and E) and in the epicuticular wax crystal images of the *ltpg1* stems and siliques that were obtained using scanning electron microscopy (data not shown).

When the *ltpg1* mutant was complemented by introduction of an approximately 3.8-kb *LTPG1* genomic clone (Supplemental Fig. S2), the altered cuticular wax phenotype was rescued. Indeed, the cuticular wax components, including C29 alkane and the C29 secondary alcohol and C29 ketone, were completely recovered in these plants (Fig. 5, A and D).

Interestingly, evaluation of the cutin monomers, which are the major extracellular lipid components, revealed no significant differences in the total amounts and chemical composition of the wild type and the *ltpg1* mutant, except approximately 3 mass % increases of C16, C18, and C18:1 dicarboxylic fatty acids in leaves (Fig. 6). Consistent with these results, the *ltpg1* leaves were not stained by 0.05% toluidine blue-O, which was used to determine the permeability of leaf cuticles that contained altered cuticular polyester (Bessire et al., 2007).

Alteration of the Cuticular Layer Structure and Accumulation of Intracellular Vesicles and Plastoglobules in the *ltpg1* Mutant

The observed alteration of the cuticular lipid composition in the *ltpg1* mutant prompted us to evaluate the ultrastructure of *ltpg1* mutants. Briefly, the wild-type and *ltpg1* mutant stems and leaves were fixed and embedded in LR White Resin. Thin sections were then stained and examined with a transmission electron microscope. Protrusions of the cytoplasm into the vacuole were observed in the stem and leaf epidermal cells of the *ltpg1* mutant (Fig. 7, A–D). Interestingly, the grana and stroma lamellae were disorganized and the size and number of plastoglobules were higher in the chloroplasts of the stem cortex of the *ltpg1* mutant (Fig. 7, E–G). A similar observation was also detected in the ultrastructure of epidermis and mesophyll cells of *ltpg1* mutant leaves. Many unidentified darkly stained deposits or vesicles were detected in the cytosol or vacuoles of the epidermis and mesophyll cells of the *ltpg1* mutant (Fig. 7, H–J). When the cuticle layer of the stem epidermis was magnified, the wild-type cuticle was found to be thin and continuously electron dense, whereas the mutant cuticle was disorganized and more diffuse (Fig. 7, K–L).

The *ltpg1* Mutant Showed Increased Susceptibility to the Fungal Pathogen *Alternaria brassicicola*

Because alteration of the ultrastructure of leaf epidermis and mesophyll cells was observed in the *ltpg1* mutant, it was further evaluated to determine if its responses to infection by the necrotrophic fungus *Alternaria brassicicola* were altered. To accomplish this, ecotype Columbia (Col-0) was used as a natural wild-type ecotype that was resistant to *A. brassicicola*. When the leaves of Arabidopsis are inoculated with fungal spores, the spores begin to germinate and form appressoria and mycelia (hyphal network), which then penetrate the host and eventually colonize the tissue (McRoberts and Lennard, 1996). As shown in Figure 8A, inoculation of Col-0 with *A. brassicicola* resulted in the formation of small brown necrotic lesions. Conversely, the *ltpg1* plants developed broad, spreading lesions upon inoculation. Lactophenol-aniline blue staining revealed that those spreading lesions were heavily colonized by fungal hyphae (Fig. 8B).

DISCUSSION

It was earlier suggested that plant LTPs are involved in intracellular lipid transport from the chloroplast to the ER and vice versa; however, the presence of a signal sequence in all members of this family led to later hypotheses that these abundant proteins may participate in the transport of cuticular lipids (wax or cutin monomers) from the plasma membrane to the cell surface through the hydrophilic cell wall matrix (Somerville et al., 2000). In this study, we identified a novel GPI-anchored LTP, LTPG1, which contributed to cuticular lipid accumulation based on the following evidence. (1) The *LTPG1* gene is expressed in the epidermis, where cuticular lipid biosynthesis may occur exclusively. (2) The LTPG1 protein is located to the plasma membrane. (3) Disruption of the *LTPG1* gene causes alteration in the cuticular lipid composition, accumulation of unidentified intracellular vesicles, alteration of the cuticular layer structure, and an increase in the size and number of plastoglobules. (4) The *ltpg1* knockout mutant showed increased susceptibility to the fungal pathogen *A. brassicicola*.

Arabidopsis epidermal microarray analysis identified seven LTPs that may be involved in the transport

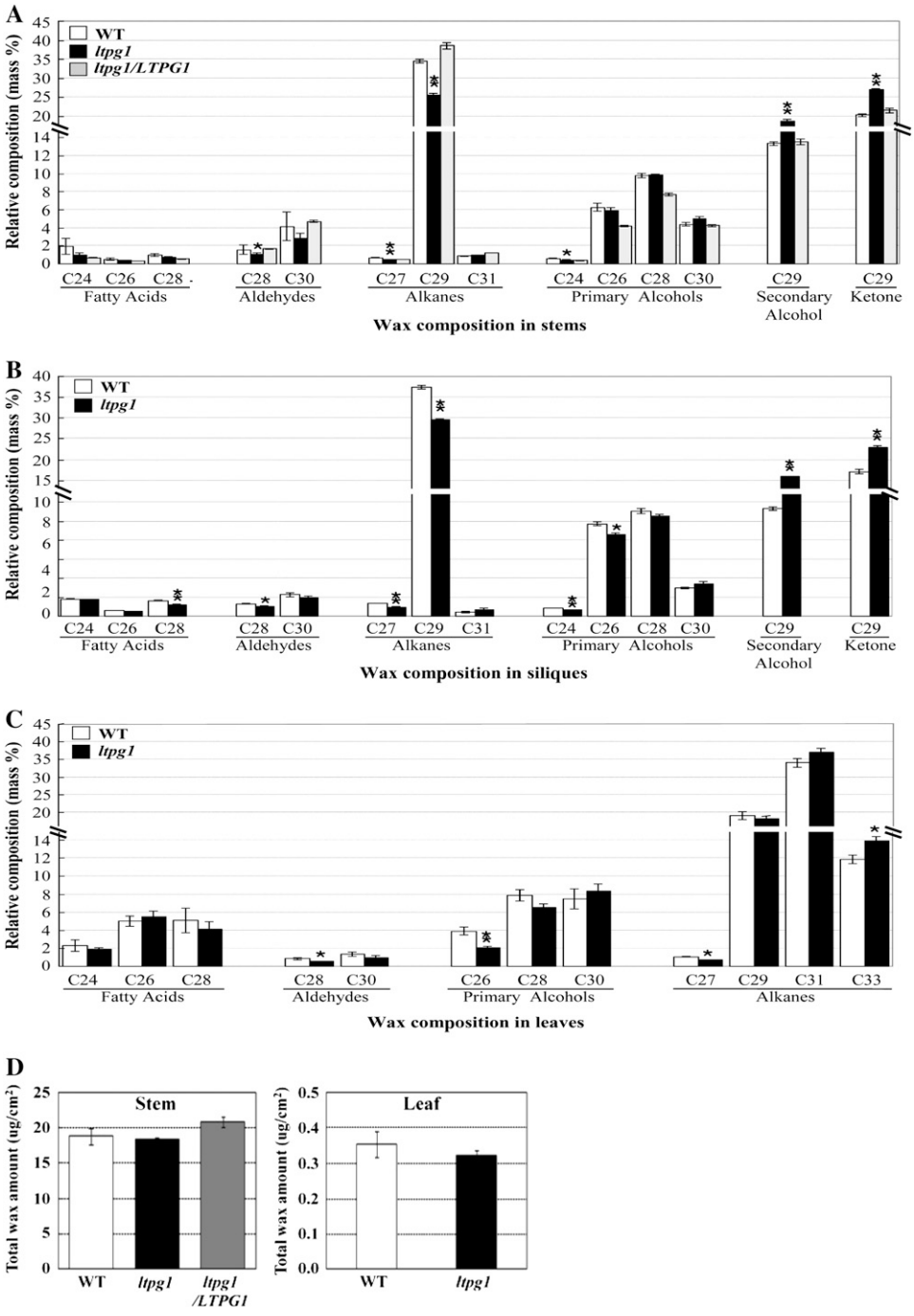

Figure 5. Cuticular wax composition (A–C) and amount (D and E) of the wild type (WT; white bars), the *ltpg1* mutant (black bars), and *ltpg1* complemented with the *LTPG1* genomic DNA (gray bars). Cuticular waxes were extracted from stems (A and D), siliques (B), and leaves (C and E) of 5- to 6-week-old Arabidopsis plants. Each value is the mean of six independent measurements ± SE. Asterisks denote statistical differences with respect to the wild-type (* $P < 0.05$, ** $P < 0.01$).

of wax and/or cutin monomers (Suh et al., 2005). One of these LTPs (At1g27950; LTPG1) was identified as a GPI-anchored protein by the following evidence. The LTP protein was found to be dissolved in the hydrophilic aqueous phase released from the Triton X-114 detergent-rich fraction of Arabidopsis callus cells upon cleavage of the GPI anchor with phosphatidylinositol-specific phospholipase C (Borner et al., 2003). The same result was reported when proteomic analysis of the Arabidopsis plasma membrane fractions was conducted by treating the samples with phospholipase D, which cleaves the anchor of the GPI-anchored

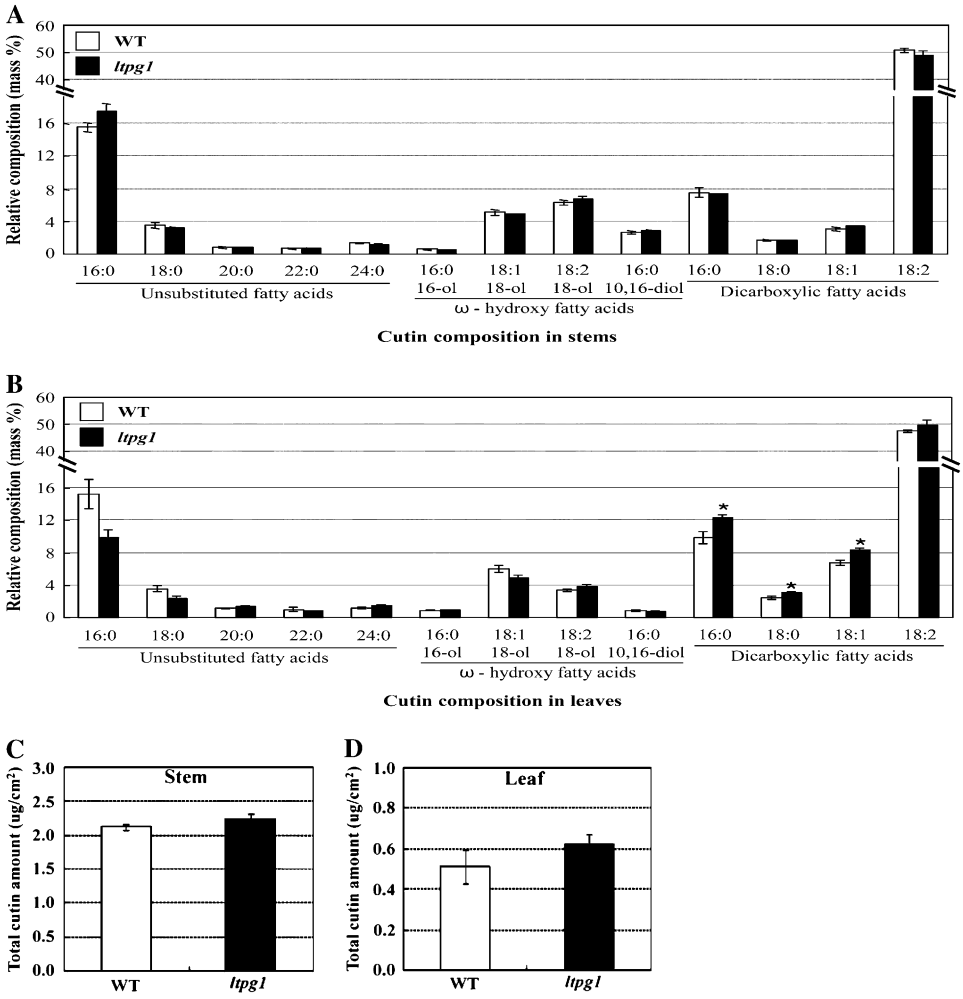

Figure 6. Cutin monomer composition (A and B) and amount (C and D) of the wild type (WT; white bars) and the *ltpg1* mutant (black bars). Cutin monomers were extracted from stems (A and C) and leaves (B and D) of 5- to 6-week-old Arabidopsis plants. Each value is the mean of three independent measurements ± SE. Asterisks denote statistical differences with respect to the wild-type (* $P < 0.05$).

proteins (Elortza et al., 2006). The results in Figure 3 confirm that LTPG1 is among the GPI proteins anchored to the plasma membrane. In previous studies, mutations in the anchor-attachment site or in the hydrophobic GPI-anchoring domain blocked anchor attachment and GPI-anchored protein transport from the ER to the Golgi compartment (Moran et al., 1991; Nuoffer et al., 1993). These results suggest that GPI anchoring is required for exit from the ER. Therefore, GPI anchoring of LTPG1 was evaluated to determine if it is essential for localization of the plasma membrane. Consistent with the results of previous studies, fluorescent signals from protoplasts transformed with LTPG1Δ48:RFP were restricted to the ER (Fig. 3, E–H), which demonstrates that GPI anchoring of the LTPG1 protein act as an ER exit signal.

GPI-anchored proteins share common structural features such as the absence of transmembrane domains, the presence of a cleavable N-terminal hydrophobic secretion signal (8–20 hydrophobic amino acid residues), and the presence of a hydrophilic spacer region that precedes the hydrophobic region in the C terminus. During posttranslational modification of GPI-anchored proteins in the lumen of the ER, a transamidase recognizes and cleaves the C-terminal hydrophobic region at the omega site. An amide linkage between the ethanolamine of the GPI anchor and the newly generated carboxyl group at the end of the cleaved protein precursor is then created (Udenfriend and Kodukula, 1995; Elortza et al., 2006). As shown in Figure 1, B and C, the LTPG1 protein harbors common structural features of the GPI-anchored proteins, which include the following: (1) an N-terminal secretion domain (amino acid residues 1–22); (2) a hydrophilic spacer region (amino acid residues 162–167); and (3) hydrophobic residues (168–191) at the C terminal end. In the LTPG1 protein, the Ala at residue 161 was predicted to be the most likely omega cleavage

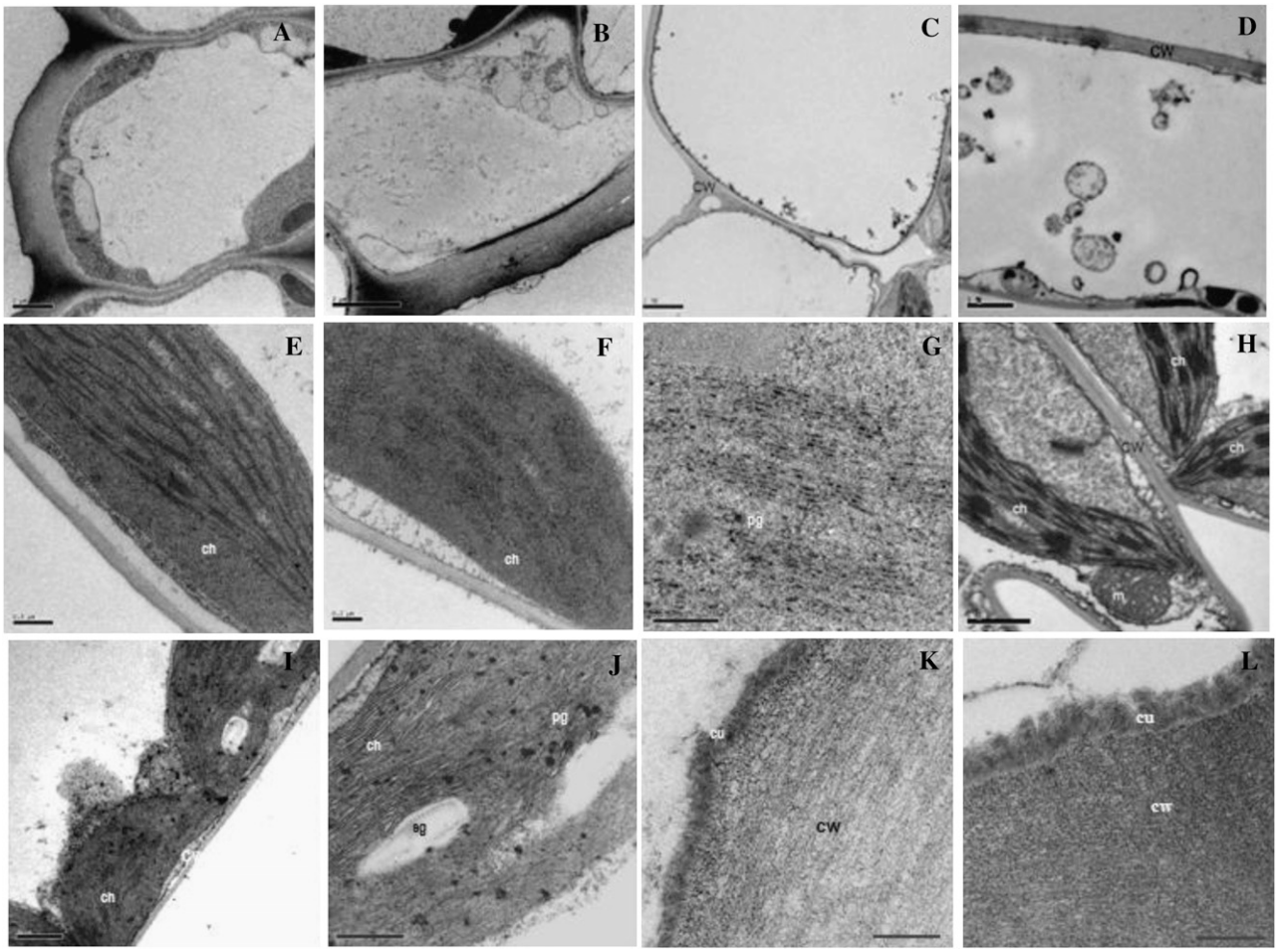

Figure 7. Transmission electron micrographs of wild-type and *ltpg1* mutant plants. A and B, Stem epidermal cells of the wild type (A) and the *ltpg1* mutant (B). C and D, Leaf epidermal cells of the wild type (C) and the *ltpg1* mutant (D). E and F, Stem cortex chloroplasts of the wild type (E) and the *ltpg1* mutant (F). G, High-magnification image of F. H and I, Leaf mesophyll cell chloroplasts of the wild type (H) and the *ltpg1* mutant (I). J, High-magnification image of (I). K and L, Cuticle layers of the wild type (K) and the *ltpg1* mutant (L). Transmission electron microscopy analysis was repeated three times. ch, Chloroplast; cu, cuticle; cw, cell wall; m, mitochondrion; pg, plastoglobule; sg, starch granule. Bars = 2 μm (A–C), 1 μm (D, H, and I), 0.5 μm (E and J), and 0.2 μm (F, G, K, and L).

site (Borner et al., 2003). However, the fluorescent signal was detected when EYFP was integrated between residues 162 and 163 (Fig. 3C), which indicates that the Ala at residue 163 or the Asp at residue 165 may be the omega cleavage site. Further study is necessary to determine if the GPI core structure of the LTPG1 is modified by the addition of extra sugars or ethanolamine phosphates, acylation of the inositol ring, changes in the fatty acids (length, saturation, and hydroxylation), or the exchange of lipid backbone diacylglycerol with ceramide.

According to the genomic and proteomic analyses, Arabidopsis harbors at least 26 LTPs with N- or C-terminal signal peptides that correspond to the GPI-anchored motif (Borner et al., 2003). However, only one of these LTPs (AtXYP1; At5g64080) has been identified to date. The AtXYP1 protein, which harbors both arabinogalactan protein and nonspecific LTP properties, is known to be involved in the differentiation of vascular tissue (Motose et al., 2004). In this study, an additional GPI-anchored LTP was investigated by characterization of an *ltpg1* knockout mutant. Disruption of the *LTPG1* gene was found to cause alterations of the cuticular lipid composition and cuticular layer structure and accumulation of intracellular vesicles (Figs. 5–7). Similar results except total wax or cutin monomer loads were observed in Arabidopsis mutants, which are deficient in the plasma membrane-localized ABC transporters CER5 and ABCG11/WBC11 (Pighin et al., 2004; Bird et al., 2007). Arabidopsis *cer5* mutants were found to have reduced stem cuticular wax loads and accumulated sheet-like inclusions in the cytoplasm of the epidermis, which suggests that CER5 is involved in wax export to the plant cuticle (Pighin et al., 2004). Additionally, Arabidopsis *wbc11* knockout mutants were shown to

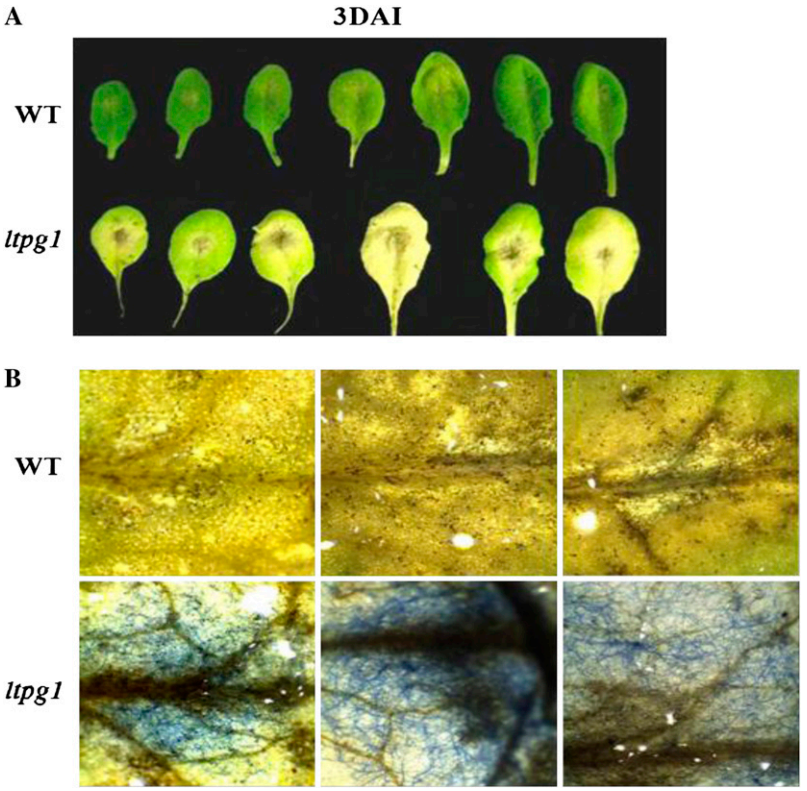

Figure 8. Disease development in *ltpg1* mutants inoculated with *A. brassicicola*. At 3 d after inoculation (DAI), necrotic lesion phenotypes (A) and necrotic lesions (B) stained with lactophenol-aniline blue were visualized with a light microscope (L2; Leica). WT, Wild type.

have lipidic inclusions inside epidermal cells and greatly reduced levels of wax and cutin, which indicates that ABCG11/WBC11 may function in cutin formation as well as in the secretion of surface waxes (Bird et al., 2007).

The LTPG1 protein harbors the LTP domain, which contains eight highly conserved Cys residues. These Cys residues are involved in the formation of disulfide bonds, which are essential for the lipid-binding property of LTPs. Plant LTPs are able to transfer phospholipids, galactolipids, fatty acids, and acyl-CoAs in vitro (Kader, 1996). In addition, the xylogen ZeXYP1 harboring a nonspecific LTP domain purified from a *Zinnia elegans* cell culture was reported to bind specifically with stigmasterol (Motose et al., 2004). In vitro assays showed that recombinant LTPG1 has lipid-binding capacity (the fluorescent lipophilic probe 2-*p*-toluidinonaphthalene-6-sulfonate; L. Samuels, personal communication). These findings raise two questions regarding the role of LTPG1, which contributes to the cuticular lipid accumulation. First, it is important to determine if the LTPG1 plays a role in the transport of specific lipids or fatty acids. In this study, significant reduction of the C29 alkane was observed in the wax composition of *ltpg1* in the stem and siliques (Fig. 5, A and B). Therefore, further investigation is necessary to determine if LTPG1 located on the plasma membrane facilitates the export of wax precursor molecules by either association with ABC transporters such as CER5 and WBC11 (Pighin et al., 2004; Bird et al., 2007) or other unknown mechanisms. Second, it would be interesting to determine if LTPG1 is indirectly associated with vesicles containing the lipid molecules that are transported. It is believed that wax precursor molecules are exported by a vesicular pathway from the ER to the plant surface (Kunst and Samuels, 2003); therefore, LTPG1 may be involved in vesicle trafficking or export.

One interesting phenotype of the *ltpg1* mutant was the accumulation of plastoglobules in the chloroplasts of the stem cortex and leaf mesophyll cells (Fig. 7). This result was supported by the expression of LTPG1 in cortex and mesophyll cells (Fig. 3). However, these phenomena were not observed in the Arabidopsis *cer5* and *wbc11* mutants, which were deficient in cuticular lipid export. Plastoglobules are lipid bodies formed as a result of a "blistering" of the stroma-side leaflet of the thylakoid membrane (Yao et al., 1991; Austin et al., 2006). The size and number of plastoglobules change during plastid development and differentiation as well as under stress conditions. Especially, the size and number of plastoglobules increases during up-regulation of the plastid lipid metabolism in response to light or oxidative stresses and during senescence (Austin et al., 2006; Bréhélin et al., 2007). Therefore, the accumulation of plastoglobules in the *ltpg1* mutant as versatile lipid sinks likely occurs via abnormal wax or cutin monomer deposition. However, this phenomenon could also occur in response to exposure to continuous environmental stresses during the growth

and development of the *ltpg1* mutants with impaired cuticle layers (Figs. 5–7).

As shown in Figure 7, alteration of the cuticular layer structure was observed in the *ltpg1* mutants. In addition, the *ltpg1* mutants showed increased susceptibility to the nonhost fungal pathogen *A. brassicicola* (Fig. 8). These results are consistent with similar observations on the Arabidopsis *gpat4/gpat8* mutant lacking glycerol-3-phosphate acyltransferase (GPAT4 and GPAT8) activity, which is essential for cutin biosynthesis (Li et al., 2007). It has been reported that Ser esterases with cutinolytic activities were only expressed during initial contact between *A. brassicicola* conidia and cutin on host surfaces that did not contain wax (Fan and Köller, 1998), which also supports our observations. Taken together, the current findings and the results of previously conducted studies suggest that formation of a normal cuticle layer is essential to prevent plants from being attacked by pathogens. In addition, it was reported that putative LTP is involved in long-distance signaling during acquisition of systemic acquired resistance in Arabidopsis (Maldonado et al., 2002). To identify a role of LTPG1 in defense signaling to the infection of pathogens, the bacterial pathogen *Pseudomonas syringae* was inoculated on the leaves of wild-type and *ltpg1* plants. No significant differences for necrotic lesion phenotypes and bacterial growth were observed (data not shown), suggesting that LTPG1 may not be involved in the plant defense response. However, it could not be excluded that LTPG1 probably functions in lipid signaling for plant defense against fungal pathogen attack.

Overall, characterization of the T-DNA-inserted *ltpg1* mutants has provided evidence that plant GPI-anchored LTP is a novel protein that contributes to cuticular lipid accumulation either directly or indirectly. It is expected that the results presented here will provide direction for future studies conducted to elucidate the mechanism by which intracellular lipids are exported to the surfaces of plants for cuticle biosynthesis.

MATERIALS AND METHODS

Plant Materials

Arabidopsis (*Arabidopsis thaliana* Col-0) was grown in the Arabidopsis room under a 16-h-light/8-h dark cycle. Seeds were sterilized in 70% (v/v) ethanol for 1 min and then in 20% (v/v) bleach for 5 min, after which they were rinsed with sterilized water. The sterilized seeds were then aseptically germinated on 0.8% (w/v) half-strength MS agar medium supplemented with 1% (w/v) Suc. To induce abiotic stresses and apply the stress hormone ABA, 10-d-old seedlings were incubated in MS liquid medium supplemented with 1 μM ABA, 20% (w/v) polyethylene glycol, 200 mM NaCl, or 200 mM mannitol for 6 h.

Genetic Analysis

Crosses were performed by emasculating the unopened buds and using the pistils as recipients for pollen. The homozygous *ltpg1* mutant was reciprocally crossed with wild-type Col-0 plants. After harvesting, the crossed seeds were grown until the F2 seeds were harvested. Because the *ltpg1* mutant is resistant to phosphinothricin, genetic segregation of F2 seeds was conducted by germinating the seeds on half-strength MS agar medium supplemented with 4 μg mL^{-1} (w/v) phosphinothricin.

RNA Isolation, RT-PCR Analysis, and Real-Time RT-PCR Analysis

Total RNA was isolated from various Arabidopsis tissues using TRIzol reagent (Sigma) according to the manufacturer's instructions. RT was conducted following the manufacturer's protocols (Invitrogen). PCR was then performed using the gene-specific primers shown in Supplemental Table S2. For the quantitative analysis of RNA transcripts by real-time RT-PCR, the transcript levels in stem and epidermis were determined in the Rotor-Gene 2000 real-time thermal cycling system (Corbett Research) using the QuantiTect SYBR Green RT-PCR kit (Qiagen) as described previously.

Construction of Binary Vectors and Arabidopsis Transformation

For isolation of the 5′ flanking regions of the *LTPG1* gene, chromosomal DNA was isolated from 10-d-old Arabidopsis seedlings using the method described by Weigel and Glazebrook (2002). Approximately 2.2 kb of the 5′ flanking region of the *LTPG1* gene was then amplified by PCR using the LTPG1 GUS F1/LTPG1 GUS R1 primers. The isolated 5′ flanking regions of the *LTPG1* gene were then digested using the *Xba*I/*Sma*I restriction enzymes, after which they were ligated into the *Xba*I/*Sma*I-digested pBI101 vector (Jefferson et al., 1987).

For complementation of the *atltpg-1* mutants, *LTPG1* genomic DNAs (approximately 3.8 kb) covering promoter, coding, and noncoding regions of the *LTPG1* gene were amplified by PCR using the LTPG1 GUS F1/LTPG1 R3 primers. The *Xba*I/*Sma*I-digested genomic DNA fragments were cloned into *Xba*I/*Sma*I-digested pBIN19 vector (Bevan, 1984).

The constructed binary vectors were transformed into *Agrobacterium tumefaciens* strain GV3101 via the freeze-thaw method (An, 1987). The Arabidopsis wild-type Col-0 was then transformed using the vacuum infiltration method described by Bechtold et al. (1993). Seeds that had been bulk harvested from each pot were then sterilized and germinated on half-strength MS agar medium supplemented with 50 μg mL^{-1} (w/v) kanamycin. T1 or T2 seedlings that survived were subsequently transferred to soil and used for further analyses.

Histochemical Analysis of GUS

Histochemical analysis of GUS activity was conducted using the method described by Jefferson et al. (1987). Briefly, developing siliques, leaves, caulines, flowers, stems, and roots were hand cut with a sharp razor and then incubated immediately in GUS staining buffer (100 mM sodium phosphate, pH 7.0, 1 mM 5-bromo-4-chloro-3-indolyl-β-D-glucuronide, 0.5 mM potassium ferrocyanide, 0.5 mM potassium ferricyanide, 10 mM Na_2EDTA, and 0.1% [v/v] Triton X-100) for 16 h at 37°C. The stained tissues were then rinsed with a graded ethanol series until pigments such as chlorophyll had been completely cleared. Next, the images were photographed using a Leica L2 microscope. To visualize the cross-sections of stems and leaves, dehydrated samples were embedded in acrylic resin (LR White Resin; London Resin Company) and then sliced into 2-mm sections using an ultramicrotome (Research Manufacturing Company). The tissue sections were then observed with a light microscope (L2; Leica).

Ultrastructure Analysis Using Transmission Electron Microscopy

The upper parts of 10-cm-long stems and leaves of 4- to 5-week-old plants were used for transmission electron microscopy analysis. Arabidopsis wild-type and *ltpg1* stems and leaves were fixed in a solution containing 2.5% glutaraldehyde and 4% paraformaldehyde in 0.1 M phosphate buffer (pH 7.4) at 4°C for 4 h. They were then rinsed in 0.1 M phosphate buffer (pH 7.4) and further fixed in 1% (w/v) OsO_4 for 4 h at 4°C. After rinsing with 0.1 M phosphate buffer, the samples were dehydrated and embedded in LR White Resin (London Resin Company). Thin sections (50 to 60 nm thick) were then prepared with an ultramicrotome (RMC MT X) and collected on nickel grids

(1-GN, 150 mesh). Next, these sections were stained with uranyl acetate and lead citrate and examined with a transmission electron microscope (Philips; Tecnai 12).

Wax Analysis

The cuticular waxes were extracted by immersing 10-cm inflorescence stems or leaves in 5 mL of chloroform at room temperature for 30 s. *n*-Octacosane, docosanoic acid, and 1-tricosanol were added as internal standards. The solvent was then removed by heating the sample to 40°C under a gentle stream of nitrogen. The remaining wax mixtures were treated with bis-*N*,*N*-(trimethylsilyl)trifluoroacetamide (Sigma) in pyridine (20 min at 100°C) to transform all of the hydroxyl-containing compounds into their corresponding trimethylsilyl derivatives. The qualitative composition was then evaluated by capillary GC-MS (GCMS-QP2010; Shimazu; column, 60 m HP-5, 0.32 mm i.d., film thickness = 0.25 μm; Agilent) using a helium carrier gas inlet pressure of 1.0 mL min^{-1} and a mass spectrometric detector (GCMS-QP2010; Shimazu). The GC-MS protocol was as follows: injection at 220°C, maintenance of the temperature at 220°C for 4.5 min followed by an increase to 290°C at a rate of 3°C min^{-1}. The temperature was then maintained at 290°C for 10 min, after which it was raised to 300°C at a rate of 2°C min^{-1} and held for 10 min. Quantitative analysis of the mixtures was performed using capillary GC with a flame ionization detector under the same GC conditions described above. Single compounds were quantified against the internal standard by automatically integrating the peak areas.

Polyester Analysis

Twenty- to 25-cm-long primary stems and leaves of 5- to 6-week-old Arabidopsis plants were used for each replicate. The analysis of the polyesters was conducted using the method described by Bonaventure et al. (2004). Internal standards were methyl heptadecanoate and ω-pentadecalactone (Sigma). Polyesters from dried solvent-extracted residues of stems and leaves were depolymerized by hydrogenolysis with methanolysis with $NaOCH_3$. The products recovered after hydrogenolysis were separated and quantified by GC-MS. The GC-MS protocol was as follows: injection at 110°C, raised by 2.5°C min^{-1} to 300°C, and held for 3 min at 300°C.

Fungal Pathogen Treatments

Inoculation with *Alternaria brassicicola* was conducted by applying a 10-μL drop of spore suspension (1×10^6 spores mL^{-1}) to each leaf of 4-week-old plants. For microscopic analyses, the lesions and fungal hyphae were visualized by staining the infected leaves using a previously described method (Kumar et al., 2004). Leaves were detached 3 d after inoculation and then stained with lactophenol-aniline blue. Lactophenol was prepared by mixing phenol:acetic acid:distilled water:glycerol (1:1:1:2, v/v/v/v). Aniline blue (0.1%, w/v) and lactophenol were then mixed at a ratio of 1:3 (Koch and Slusarenko, 1990). The stained samples were mounted in 60% glycerol and examined using a light microscope (L2; Leica).

EYFP Tagging and Subcellular Localization of LTPG1

EYFP was amplified by PCR using the p35S-EYFP-Flag/Strep plasmid as a template and the YFP-F1/YFP-R1 primers. The full-length *LTPG1* cDNA was used to amplify the *LTPG1* cDNA1 and *LTPG1* cDNA2 fragments using the LTPG1 cDNA F2/LTPG1 P1 and LTPG1 P2/LTPG1 cDNA R2 primers, respectively. A triple template PCR was then performed to produce an *LTPG1* cDNA with the EYFP following the method described by Tian et al. (2004). The triple template PCR products were digested with *Sma*I/*Bam*HI enzymes and ligated into *Sma*I/*Bam*HI-digested p35S-EYFP-Flag/Strep plasmid.

The constructed plasmids were purified using a Qiagen Plasmid Maxi kit. Protoplasts were prepared from Arabidopsis mesophyll cells and transformed with the purified plasmid DNA by polyethylene glycol-mediated protoplast transformation as described previously (Abel and Theologis, 1998). The transformed protoplasts were then incubated for 18 h in darkness at room temperature, after which the fluorescence was observed using a Nikon Eclipse TE2000-U microscope.

For transient expression in tobacco (*Nicotiana tabacum* 'Xanthi') leaf epidermis, the abaxial side of tobacco leaves was injected with *Agrobacterium* strain GV3101 harboring the LTPG1:EYFP plasmid using a 1-mL syringe without a needle (Sparkes et al., 2006). Transient expression was examined to epidermis at the lower surface of the leaves. YFP fluorescence was examined 48 to 60 h after injection. YFP fluorescence and propidium iodide fluorescence were analyzed in a TCS SP5 AOBS/Tandem laser confocal scanning microscope (Leica) with excitation at 458, 561, 594, and 633 nm produced by an argon/diode-pumped solid-state/helium-neon ion laser.

Supplemental Data

The following materials are available in the online version of this article.

Supplemental Figure S1. Expression of the *LTPG1* transcripts in various tissues (A) and 10-d-old seedlings after exogenous applications of abiotic stresses and the stress hormone ABA (B).

Supplemental Figure S2. Complementation of the *ltpg1* mutants by introduction of the *LTPG1* genomic clone.

Supplemental Table S1. Phosphinothricin resistance of F2 progeny of the *ltpg1* heterozygotes (F1), which were generated by crossing the *ltpg1* mutant with the wild type.

Supplemental Table S2. Oligonucleotide sequences used in this study.

ACKNOWLEDGMENTS

We thank Syngenta Arabidopsis Insertion Library resources (http://www.tmri.org/en/site/home.aspx) for providing T-DNA-tagged *ltpg1* (Garlic_1166_G01.b.1a.Lb3Fa) Arabidopsis mutants. We also thank Jeong Sheop Shin at Korea University for providing the p35S-EYFP-Flag/Strep plasmid, Hyo Jin Kim at Chonnam National University for technical support, and John Ohlrogge at Michigan State University for critical review of the manuscript. Acknowledgment is also made of the Korea Basic Science Institute, Gwangju Center, for the confocal microscopy and image analysis.

Received February 25, 2009; accepted March 19, 2009; published March 25, 2009.

LITERATURE CITED

Aarts MGM, Keijzer CJ, Stiekema WJ, Pereira A (1995) Molecular characterization of the CER1 gene of *Arabidopsis* involved in epicuticular wax biosynthesis and pollen fertility. Plant Cell **7:** 2115–2127

Abel S, Theologis A (1998) Transient gene expression in protoplasts of *Arabidopsis thaliana*. Methods Mol Biol **82:** 209–217

An G (1987) Binary Ti vector for plant transformation and promoter analysis. Methods Enzymol **153:** 292–305

Austin JR II, Frost E, Vidi PA, Kessler F, Staehelin LA (2006) Plastoglobules are lipoprotein subcompartments of the chloroplast that are permanently coupled to thylakoid membranes and contain biosynthetic enzymes. Plant Cell **18:** 1693–1703

Baker CJ, McCormick SL, Bateman DF (1982) Effects of purified cutin esterase upon the permeability and mechanical strength of cutin membranes. Phytopathology **72:** 420–423

Bechtold N, Ellis J, Pelletier G (1993) *In planta Agrobacterium*-mediated gene transfer by infiltration of adult Arabidopsis thaliana plants. C R Acad Sci Paris Life Sci **316:** 1194–1199

Beisson F, Koo AJ, Ruuska S, Schwender J, Pollard M, Thelen JJ, Paddock T, Salas JJ, Savage L, Milcamps A, et al (2003) Arabidopsis gene involved in acyl lipid metabolism: a 2003 census of the candidates, a study of the distribution of expressed sequence tags in organs, and a Web-based database. Plant Physiol **132:** 681–697

Bessire M, Chassot C, Jacquat AC, Humphry M, Borel S, Petétot JMC, Métraux JP, Nawrath C (2007) A permeable cuticle in Arabidopsis leads to a strong resistance to *Botrytis cinerea*. EMBO J **26:** 2158–2168

Bevan MW (1984) Binary *Agrobacterium* vectors for plant transformation. Nucleic Acids Res **12:** 8711–8721

Bird D, Beisson F, Brigham A, Shin J, Greer S, Jetter R, Kunst L, Wu X, Yephremov A, Samuels L (2007) Characterization of Arabidopsis

ABCG11/WBC11, an ATP binding cassette (ABC) transporter that is required for cuticular lipid secretion. Plant J **52:** 485–498

Bonaventure G, Beisson F, Ohlrogge J, Pollard M (2004) Analysis of the aliphatic monomer composition of polyesters associated with Arabidopsis epidermis: occurrence of octadeca-cis-6,cis-9-diene-1,18-dioate as the major component. Plant J **40:** 920–930

Borner GHH, Lilley KS, Stevens TJ, Dupree P (2003) Identification of glycosylphosphatidylinositol-anchored proteins in Arabidopsis: a proteomic and genomic analysis. Plant Physiol **132:** 568–577

Bréhélin C, Kessler F, van Wijk KJ (2007) Plastoglobules: versatile lipoprotein particles in plastids. Trends Plant Sci **12:** 260–266

Cameron KD, Teece MA, Smart LB (2006) Increased accumulation of cuticular wax and expression of lipid transfer protein in response to periodic drying events in leaves of tree tobacco. Plant Physiol **140:** 176–183

Choi AM, Lee SB, Cho SH, Hwang I, Hur CG, Suh MC (2008) Isolation and characterization of multiple abundant lipid transfer protein isoforms in developing sesame (*Sesamum indicum* L.) seeds. Plant Physiol Biochem **46:** 127–139

Clemens S, Kunst L, inventors. January 2, 2001. Plant long chain fatty acid biosynthetic enzyme. European Patent Application WO 0107586

Dietrich CR, Perera MA, D Yandeau-Nelson M, Meeley RB, Nikolau BJ, Schnable PS (2005) Characterization of two GL8 paralogs reveals that the 3-ketoacyl reductase component of fatty acid elongase is essential for maize (*Zea mays* L.) development. Plant J **42:** 844–861

Elortza F, Mohammed S, Bunkenborg J, Foster LJ, Nühse TS, Brodbeck U, Peck SC, Jensen ON (2006) Modification-specific proteomics of plasma membrane proteins: identification and characterization of glycosylphosphatidylinositol-anchored proteins released upon phospho-lipase D treatment. J Proteome Res **5:** 935–943

Fan CY, Köller W (1998) Diversity of cutinases from plant pathogenic fungi: differential and sequential expression of cutinolytic esterases by *Alternaria brassicicola*. FEMS Microbiol Lett **158:** 33–38

Fiebig A, Mayfield JA, Miley NL, Chau S, Fischer RL, Preuss D (2000) Alterations in *CER6*, a gene identical to *CUT1*, differentially affect long-chain lipid content on the surface of pollen and stems. Plant Cell **12:** 2001–2008

Heredia A (2003) Biophysical and biochemical characteristics of cutin, a plant barrier biopolymer. Biochim Biophys Acta **1620:** 1–7

Hoffmann-Benning S, Kende H (1994) Cuticle biosynthesis in rapidly growing internodes of deepwater rice. Plant Physiol **104:** 719–723

Holloway PJ (1982) Structure and histochemistry of plant cuticular membranes: an overview. *In* The Plant Cuticle. Academic Press, London, pp 1–32

Hooker TS, Millar AA, Kunst L (2002) Significance of the expression of the CER6 condensing enzyme for cuticular wax production in Arabidopsis. Plant Physiol **129:** 1568–1580

Jefferson RA, Kavanagh TA, Bevan MW (1987) GUS fusions: β-glucuronidase as a sensitive and versatile gene fusion marker in higher plants. EMBO J **6:** 3901–3907

Jeffree CE (1996) Structure and ontogeny of plant cuticles. *In* G Kerstiens, ed, Plant Cuticles: An Integrated Functional Approach. BIOS Scientific Publishers, Oxford, pp 33–82

Jenks MA, Eigenbrode S, Lemieux B (2002) Cuticular waxes of Arabidopsis. *In* CR Somerville, EM Meyerowitz, eds, The Arabidopsis Book. American Society of Plant Biologists, Rockville, MD, doi/10.1199/tab.0016, http://www.aspb.org/publications/arabidopsis/

Jeroen N, Feron R, Huisman BAH, Fasolino A, Hilbers CW, Derksen J, Mariani C (2005) Lipid transfer proteins enhance cell wall extension in tobacco. Plant Cell **17:** 2009–2019

Kader JC (1996) Lipid-transfer proteins in plants. Annu Rev Plant Physiol Plant Mol Biol **47:** 627–654

Koch E, Slusarenko AJ (1990) *Arabidopsis* is susceptible to infection by a downy mildew fungus. Plant Cell **2:** 437–445

Kolattukudy PE (2001) Polyesters in higher plants. Adv Biochem Eng Biotechnol **71:** 1–49

Kumar A, Tripathi K, Rana M, Purwar S, Garg GK (2004) Dibutyryl c-AMP as an inducer of sporidia formation: biochemical and antigenic changes during morphological differentiation of Karnal bunt (*Tilletia indica*) pathogen in axenic culture. J Biosci **29:** 23–31

Kunst L, Samuels AL (2003) Biosynthesis and secretion of plant cuticular wax. Prog Lipid Res **42:** 51–80

Kunst L, Samuels AL, Jetter R (2005) The plant cuticle: formation and structure of epidermal surfaces. *In* D Murphy, ed, Plant Lipids: Biology, Utilisation and Manipulation. Blackwell Scientific, Oxford, pp 270–302

Li Y, Beisson F, Koo AJ, Molina I, Pollard M, Ohlrogge J (2007) Identification of acyltransferases required for cutin biosynthesis and production of cutin with suberin-like monomers. Proc Natl Acad Sci USA **104:** 18339–18344

Lolle SJ, Hsu W, Pruitt RE (1998) Genetic analysis of organ fusion in *Arabidopsis thaliana*. Genetics **149:** 607–619

Luo B, Xue XY, Hu WL, Wang LJ, Chen XY (2007) An ABC transporter gene of *Arabidopsis thaliana*, AtWBC11, is involved in cuticle development and prevention of organ fusion. Plant Cell Physiol **48:** 1790–1802

Maldonado AM, Doerner P, Dixon RA, Lamb CJ, Cameron RK (2002) A putative lipid transfer protein involved in systemic resistance signaling in Arabidopsis. Nature **419:** 399–403

Mayor S, Riezman H (2004) Sorting GPI-anchored proteins. Nat Rev Mol Cell Biol **5:** 110–120

McRoberts N, Lennard JH (1996) Pathogen behaviour and plant cell reactions in interactions between Alternaria species and leaves of host and nonhost plants. Plant Pathol **45:** 742–752

Millar AA, Clemens S, Zachgo S, Giblin EM, Taylor DC, Kunst L (1999) *CUT1*, an *Arabidopsis* gene required for cuticular wax biosynthesis and pollen fertility, encodes a very-long-chain fatty acid condensing enzyme. Plant Cell **11:** 825–838

Millar AA, Kunst L (1997) Very-long-chain fatty acid biosynthesis is controlled through the expression and specificity of the condensing enzyme. Plant J **12:** 121–131

Min MK, Kim SJ, Miao Y, Shin JY, Jiang L, Hwang I (2007) Overexpression of Arabidopsis AGD7 causes relocation of Golgi-localized proteins to the endoplasmic reticulum and inhibits protein trafficking in plant cells. Plant Physiol **143:** 1601–1614

Molina A, García-Olmedo F (1997) Enhanced tolerance to bacterial pathogens caused by the transgenic expression of barley lipid transfer protein LTP2. Plant J **12:** 669–675

Moran P, Raab H, Kohr WJ, Caras IW (1991) Glycophospholipid membrane anchor attachment: molecular analysis of the cleavage/attachment site. J Biol Chem **266:** 1250–1257

Motose H, Sugiyama M, Fukuda H (2004) A proteoglycan mediates inductive interaction during plant vascular development. Nature **429:** 873–878

Nawrath C (2002) The biopolymers cutin and suberin. *In* CR Somerville, EM Meyerowitz, eds, The Arabidopsis Book. American Society of Plant Biologists, Rockville, MD, doi/10.1199/tab.0021, http://www.aspb.org/publications/arabidopsis/

Nawrath C (2006) Unraveling the complex network of cuticular structure and function. Curr Opin Plant Biol **9:** 281–287

Nuoffer C, Horvath A, Riezman H (1993) Analysis of the sequence requirements for glycosylphosphatidylinositol anchoring of *Saccharomyces cerevisiae* Gas1 protein. J Biol Chem **268:** 10558–10563

Pighin JA, Zheng H, Balakshin LJ, Goodman LP, Western TL, Jetter R, Kunst L, Samuels AL (2004) Plant cuticular lipid export requires an ABC transporter. Science **306:** 702–704

Pyee J, Kolattukudy PE (1995) The gene for the major cuticular wax-associated protein and three homologous genes from broccoli (*Brassica oleracea*) and their expression patterns. Plant J **7:** 49–59

Riederer M, Schreiber L (2001) Protecting against water loss: analysis of the barrier properties of plant cuticles. J Exp Bot **52:** 2023–2032

Rowland O, Zheng H, Hepworth SR, Lam P, Jetter R, Kunst L (2006) CER4 encodes an alcohol-forming fatty acyl-coenzyme A reductase involved in cuticular wax production in Arabidopsis. Plant Physiol **142:** 866–877

Roy-Barman S, Sautter C, Chattoo BB (2006) Expression of the lipid transfer protein Ace-AMP1 in transgenic wheat enhances antifungal activity and defense responses. Transgenic Res **15:** 435–446

Schulz B, Frommer WB (2004) A plant ABC transporter takes the lotus seat. Science **306:** 622–625

Schweizer P, Felix G, Buchala A, Muller C, Metraux JP (1996) Perception of free cutin monomers by plant cells. Plant J **10:** 331–341

Shin DH, Lee JY, Hwang KY, Kim KK, Suh SW (1995) High-resolution crystal structure of the non-specific lipid-transfer protein from maize seedlings. Structure **3:** 189–199

Sieber P, Schorderet M, Ryser U, Buchala A, Kolattukudy P, Metraux JP, Nawrath C (2000) Transgenic *Arabidopsis* plants expressing a fungal cutinase show alterations in the structure and properties of the cuticle and postgenital organ fusions. Plant Cell **12:** 721–737

Somerville C, Browse J, Jaworski JG, Ohlrogge JB (2000) Lipids. *In* BB Buchanan, W Gruissem, RL Jones, eds, Biochemistry and Molecular Biology of Plants. American Society of Plant Physiologists, Rockville, MD, pp 456–527

Sparkes IA, Runions J, Kearns A, Hawes C (2006) Rapid, transient expression of fluorescent fusion proteins in tobacco plants and generation of stably transformed plants. Nat Protocols **1:** 2019–2025

Stark RE, Tian S (2006) The cutin biopolymer matrix. *In* M Riederer, C Müller, eds, Biology of the Plant Cuticle. Blackwell Publishing, Oxford, pp 126–144

Suh MC, Samuels AL, Jetter R, Kunst L, Pollard M, Ohlrogge J, Beisson F (2005) Cuticular lipid composition, surface structure, and gene expression in Arabidopsis stem epidermis. Plant Physiol **139:** 1649–1665

Tian GW, Mohanty A, Chary SN, Li S, Paap B, Drakakaki G, Kopec CD, Li J, Ehrhardt D, Jackson D, et al (2004) High-throughput fluorescent tagging of full-length Arabidopsis gene products in planta. Plant Physiol **135:** 25–38

Todd J, Post-Beittenmiller D, Jaworski JG (1999) KCS1 encodes a fatty acid elongase 3-ketoacyl-CoA synthase affecting wax biosynthesis in *Arabidopsis thaliana*. Plant J **17:** 119–130

Udenfriend S, Kodukula K (1995) How glycosylphosphatidylinositol-anchored membrane proteins are made. Annu Rev Biochem **64:** 563–591

Weigel D, Glazebrook J (2002) Arabidopsis: A Laboratory Manual, Ed 3. Cold Spring Harbor Laboratory Press, Cold Spring Harbor, NY, pp 165–170

Yao K, Paliyath G, Humphrey RW, Hallet FR, Thompson JE (1991) Identification and characterization of nonsedimentable lipid-protein microvesicles. Proc Natl Acad Sci USA **88:** 2269–2273

Yephremov A, Wisman E, Huijser P, Huijser C, Wellesen K, Saedler H (1999) Characterization of the FIDDLEHEAD gene of *Arabidopsis* reveals a link between adhesion response and cell differentiation in the epidermis. Plant Cell **11:** 2187–2201

Zheng H, Rowland O, Kunst L (2005) Disruptions of the *Arabidopsis* enoyl-CoA reductase gene reveal an essential role for very-long-chain fatty acid synthesis in cell expansion during plant morphogenesis. Plant Cell **17:** 1467–1481